water

MDPI

Article

Assessing the Impact of Deforestation on Decadal Runoff Estimates in Non-Homogeneous Catchments of Peninsula Malaysia

Jen Feng Khor [1], Steven Lim [2], Vania Lois Ling [3] and Lloyd Ling [1,*]

[1] Centre of Disaster Risk Reduction (CDRR), Lee Kong Chian Faculty of Engineering & Science, Universiti Tunku Abdul Rahman, Jalan Sungai Long, Kajang 43000, Malaysia
[2] Centre for Photonics and Advanced Materials Research, Lee Kong Chian Faculty of Engineering & Science, Universiti Tunku Abdul Rahman, Jalan Sungai Long, Kajang 43000, Malaysia
[3] School of Banking and Finance, Asia Pacific University, Technology Park Malaysia, Kuala Lumpur 57000, Malaysia
* Correspondence: linglloyd@utar.edu.my

Abstract: This study calibrated the Soil Conservation Service Curve Number (SCS-CN) model to predict decadal runoff in Peninsula Malaysia and found a correlation between the reduction of forest area, urbanization, and an increase in runoff volume. The conventional SCS-CN runoff model was found to commit a type II error in this study and must be pre-justified with statistics and calibrated before being adopted for any runoff prediction. Between 1970 and 2000, deforestation in Peninsula Malaysia caused a decline in forested land by 25.5%, resulting in a substantial rise in excess runoff by 10.2%. The inter-decadal mean runoff differences were more pronounced in forested and rural catchments (lower CN classes) compared to urban areas. The study also found that the CN value is a sensitive parameter, and changing it by ±10% can significantly impact the average runoff estimate by 40%. Therefore, SCS practitioners are advised not to adjust the CN value for better runoff modeling results. Additionally, NASA's Giovanni system was used to generate 20 years of monthly rainfall data from 2001–2020 for trend analysis and short-term rainfall forecasting. However, there was no significant uptrend in rainfall within the period studied, and occurrences of flood and landslide incidents were likely attributed to land-use changes in Peninsula Malaysia.

Keywords: deforestation and decadal runoff predictions; urbanization; non-homogenous catchments; Peninsula Malaysia

Citation: Khor, J.F.; Lim, S.; Ling, V.L.; Ling, L. Assessing the Impact of Deforestation on Decadal Runoff Estimates in Non-Homogeneous Catchments of Peninsula Malaysia. *Water* **2023**, *15*, 1162. https://doi.org/10.3390/w15061162

Academic Editor: Mojca Šraj

Received: 11 February 2023
Revised: 12 March 2023
Accepted: 14 March 2023
Published: 17 March 2023

1. Introduction

Humans have significantly altered the earth's surface over time by transforming natural areas into industrial or agricultural regions. In the case of Malaysia, as a developing country, there has been extensive land-use and land-cover change since the 1970s. The rapid pace of development in Peninsula Malaysia has resulted in changes to the landscape and vegetation. These activities have had an uneven impact on the drainage basins, leading to changes in runoff patterns. Human activities, especially deforestation, have a greater impact on vegetation cover and the environment at local, regional, and global levels. Land-use and water cycle patterns are also influenced by anthropogenic activities, particularly deforestation, which has cleared the way for urban development. As a result, it is crucial to explore and estimate the impact of development activities on runoff patterns in rural catchments in Malaysia [1–3].

Forests are an essential element in sustaining our supply of water [4–8]. However, to make room for development, many forested areas have been cleared [9–15]. Between 2002 and 2020, Malaysia lost 27,000 km^2 (roughly 2/3 of Switzerland or nearly 39 Singapores) [16] of humid primary forest area at the clearing rate of 1421 km^2/year within

19 years. This had resulted in a 17% reduction of humid primary forest in Malaysia within the given time period [17]. Compared to the deforestation of an area of 13,000 km^2 from 1978 to 1994 [18], the forest-clearing rate in Malaysia has doubled in recent decades. Deforestation challenged the quality and quantity of water [19] and caused significant hydrological changes which included an increase in runoff [20,21].

Interception losses in tropical and subtropical rainforests have been shown to vary from 6 to 42% of rainfall [22–24]. Meanwhile in Malaysia and Indonesia, forest interception loss was reported from 12.7% to 21% [25,26]. Forest removal will convert the interception losses into a contributing factor to increase surface runoff. Past research studies have investigated rainforest conversion and its hydrological impact [27–34]. Zhang et al. [35] reported that a reduction of forest cover from 22% to 10% caused changes in river discharge in China. Sharma et al. [36] concluded that under projected land-use scenarios, runoff would increase when forest areas were converted into agricultural land in the central Himalayas.

The conversion of natural land has increased the surface runoff while rapid urbanization and industrialization have been cited as the main causes of major flooding in Malaysia [37,38]. Many researchers quantified the effects on hydrological parameters as due to changes in vegetation cover or forest logging activities [39–44], while urbanization was also identified to be a key factor in landscape alteration, causing an increase in runoff. River discharge can also be affected by human interventions. The landscape alteration caused faster runoff from storms, increased peak flows and changed hydrologic cycles [45–47]. Sahin and Hall [48] reported that a 10% reduction in canopy cover resulted in a 20 to 25 mm increase in annual water yield while Bosh and Heewlett [39] found that a 10% removal increased the water yield by an average of 40 mm. Although flooding is a response to the complex hydrological system, the dynamic changes are caused by anthropogenic factors to mother nature.

The Soil Conservation Services (SCS) of the United States has developed a widely accepted methodology, called the Curve Number (CN), to estimate the direct runoff from rainfall in hydrological studies. This method is based on the concept that the amount of runoff produced by a rainfall event depends on various factors, such as land use, soil type, and the antecedent moisture condition of the soil. The SCS-CN method uses a CN value that represents the combined effect of these factors on runoff generation, ranging from 0 to 100. This value is used in an equation to estimate the amount of direct runoff from rainfall. The SCS-CN method is commonly used in watershed management, flood forecasting, and erosion control planning, and has been widely adopted by government agencies worldwide, integrated into software, and taught in hydrology courses.

However, studies around the world in recent decades reported runoff prediction accuracy problems with the conventional SCS-CN model [49,50]. Previous studies have utilized the SCS Curve Number ($CN_{0.2}$) to demonstrate variations in runoff response due to agricultural land-use and seasonal changes [51]. This paper applied the SCS-CN model calibration methodology with inferential statistics that was developed by authors in a previous study [50] and demonstrated the extended application to model decadal rainfall-runoff conditions in Peninsula Malaysia. The correlation between deforestation and urbanization on runoff increment in Peninsula Malaysia was also established.

2. Materials and Methods

2.1. Study Site and Data Collection

Peninsula Malaysia, with a land area of 132,265 km^2, is slightly larger than England (130,395 km^2). It is bordered by Thailand to the north and Singapore across the strait of Johor to the south. This study utilized the calibrated SCS lump rainfall-runoff model in conjunction with the most recent rainfall-runoff dataset published by the Malaysian federal agency. The dataset, which can be located in the appendix of the Department of Irrigation and Drainage's Hydrological Procedures no. 27 (DID HP 27), documented 227 storm events across 41 distinct catchments between 1970 and January 2000 in Peninsula Malaysia [52]. The smallest recorded storm event had a rainfall depth of 19 mm, with a measurable runoff

depth of 4.8 mm, while the largest event measured 420 mm in rainfall depth and 258 mm in runoff depth.

In this study, the DID HP 27 dataset was divided into three periods to investigate the potential relationship between decadal runoff conditions, urban population growth in Peninsula Malaysia, and deforestation data provided by the Forestry Department Peninsula Malaysia [53–59]. This study grouped 58 recorded storm events from 1970 to 1979 as the M70 dataset, 81 events from 1980 to 1989 as the M80 dataset, and 88 events from 1990 to January 2000 as the M90 dataset for runoff analyses and comparison.

2.2. Calibration of SCS-CN Model

The SCS initially developed the CN rainfall-runoff model (Equation (1)) for the federal flood control program in 1954, and it has since become the basic model for runoff estimation.

$$Q = \frac{(P - I_a)^2}{P - I_a + S} \quad (1)$$

Q = Runoff depth (mm)
P = Rainfall depth (mm)
I_a = Rainfall initial abstraction amount (mm)
S = Catchment maximum water retention potential (mm)
where $I_a = \lambda S$. If $P < I_a$, $Q = 0$.

The SCS also put forth the hypothesis that $I_a = \lambda S = 0.2S$, where λ represents the initial abstraction ratio coefficient, which was proposed as a constant value of 0.2. The justification for Equation (1) was based on daily rainfall and runoff data, rather than event measurements, and its only official documentation source can be found in the National Engineering Handbook, Section 4 (NEH-4) [60,61]. By substituting $I_a = 0.2S$, Equation (1) is simplified into Equation (2):

$$Q = \frac{(P - 0.2S)^2}{P + 0.8S} \quad (2)$$

DID HP 27 dataset was used to assess the SCS-CN rainfall-runoff model in authors' previous study [50] with inferential statistics and concluded that the existing SCS-CN model is not even statistically significant at alpha = 0.05 level for runoff predictions in Peninsula Malaysia. Therefore, it must be calibrated according to the local rainfall-runoff dataset and the key parameter λ must be derived to formulate a statistically significant rainfall-runoff model for Peninsula Malaysia. All statistical analyses were performed using the IBM SPSS software version 26.0 in this study [62].

The SCS model was calibrated according to each decadal rainfall-runoff data batch and the calibrated runoff predictive models were formulated with the newly derived λ value to represent the aforementioned decadal rainfall-runoff conditions. Inter-decadal runoff difference can then be mapped with the runoff difference between newly formulated decadal rainfall-runoff models while non-parametric statistics were used for runoff trend analyses.

This study also re-assessed the validity of Equation (1) on the entire M70, M80, and M90 datasets through the reverse derivation of the λ value. Equation (2) will be discarded if the inferential statistics of the P-Q dataset reject the validity of $\lambda = 0.2$. Equation (1) will then be calibrated according to the P-Q data pairs of M70, M80, and M90. Non-parametric inferential statistics, bootstrapping, and Bias Corrected and Accelerated (BCa) procedure (2000 samples with replacement) were conducted in SPSS on each batch of derived λ and S values in order to search for optimum values within the confidence intervals at alpha 0.01 level. The λ confidence intervals' span can be used to assess the null hypothesis H_0 as shown below:

Null Hypothesis (H_0): Equation (2) ($\lambda = 0.2$) is valid to model runoff estimates with DID HP 27 dataset.

The SCS-CN model calibration of this study consists of the following steps:

1. Rearrange Equation (1) into: $S = \frac{(P-I_a)^2}{Q} + I_a - P$
2. For each *P*-*Q* event pair, calculate the corresponding *S* value with the above equation under the SCS constraint that $I_a < P$ value and calculate the λ value with $\lambda = I_a/S$.
3. Conduct bootstrap, BCa (at $\alpha = 0.01$ level) inferential statistical analyses (2000 samples with replacement) for the calculated λ and *S* datasets separately for each decadal model.
4. Generate 99% confidence intervals for λ and *S* datasets for each decadal model.
5. Test the null hypothesis (H_0) by referring to the λ confidence intervals' span and its standard deviation for each decadal model. If the $\lambda = 0.2$ value exists within the λ confidence interval, use Equation (2) to model rainfall-runoff. Otherwise, move to step 6.
6. Find the optimum λ and *S* values from BCa confidence intervals and calculate I_a for each decadal model using supervised optimization technique by minimizing the overall model bias (BIAS) near to the value of zero.
7. Formulate the calibrated SCS model by substituting I_a and *S* into Equation (1).
8. According to a group of researchers [63], when λ value other than 0.2 is detected, its corresponding *S* value (denoted by S_λ) must be correlated to the $S_{0.2}$ values for CN calculation. As such, correlate S_λ and $S_{0.2}$ with the *S* general formula which was derived by a past researcher [50]: $S_\lambda = \frac{\left[P - \frac{(\lambda-1)Q}{2\lambda}\right] - \sqrt{PQ - P^2 + \left[P - \frac{(\lambda-1)Q}{2\lambda}\right]^2}}{\lambda}$
9. Substitute optimum λ and S_λ into Equation (1) to formulate the decadal model.
10. Lastly, substitute $S_{0.2} = \frac{25{,}400}{CN_{0.2}} - 254$ into each decadal model to express *Q* in term of *P* and $CN_{0.2}$.

Note: Appendix B shows step 9 and 10 using an example.

2.3. IMERG Satellite Rainfall Trend Analysis

The Integrated Multi-Satellite Retrievals for Global Precipitation Measurement (IMERG) [64] is a unified satellite product that has been launched by NASA and JAXA. This product combines, calibrates, and integrates satellite microwave precipitation estimates with microwave-calibrated infrared satellite estimates, precipitation gauge analyses, and other precipitation estimators, in order to provide precipitation measurements at fine time and space scales across the globe. There are three types of IMERG systems: Early (IMERG-E), Late (IMERG-L), and Final (IMERG-F) runs, with latency times of 6 h, 18 h, and 3 months, respectively. All IMERG runs are available at half-hourly, daily, and monthly temporal resolutions, and have global coverage at a spatial resolution of 0.1°.

In this study, the IMERG-F monthly version 6 product at a spatial resolution of 0.1° was employed, as it has been bias-corrected using precipitation gauges from the Global Precipitation Climatology Centre (GPCC) and is considered more accurate for scientific research compared with other IMERG products. The data can be accessed through NASA's Giovanni system [65]. Monthly rainfall data from 2001 to 2020 (Appendix A) was obtained from the Giovanni system to demonstrate the annual rainfall distribution across Malaysia.

Trend analysis was conducted on the monthly rainfall data in Malaysia. Before conducting the analysis, a normality test was performed to determine which central of tendency (mean or median) was to be used. If a dataset has less than 2000 samples, the Shapiro-Wilk test is recommended instead of the Kolmogorov-Smirnov test. This study used a dataset with less than 2000 samples; therefore, the Shapiro-Wilk test was employed. If the *p*-value is greater than 0.05, the dataset is considered to be normally distributed, and therefore, mean is used to measure the central tendency of the dataset [50]. The non-parametric inferential statistics using the BCa bootstrapping method was conducted on 2000 random samples (with replacement) to calculate the 99% confidence intervals of the mean or median for each interval.

Rainfall time series forecasting models were created using monthly rainfall data in Malaysia from January 2001 to December 2020 (N = 240) with the Expert Modeler in SPSS. The rainfall amount was forecasted for the next 24 months, from January 2021 to December

2022 in Malaysia, to determine if there will be a significant change in rainfall pattern in the near future that could affect runoff prediction.

3. Results and Discussion

3.1. The Optimum λ and S of Decadal Models

Tables 1–3 display the BCa 99% confidence intervals of λ for the M70, M80, and M90 decadal datasets. The BCa 99% confidence intervals of both the mean and median for each decadal dataset do not include the value of 0.2, leading to the rejection of the null hypothesis (H_0) at the alpha = 0.01 level. Equation (2) was found to be statistically invalid and, thus, cannot be utilized to model runoff conditions in Peninsula Malaysia for the M70, M80, and M90 decadal datasets. The rejection of H_0 necessitates the search for a new, optimal value of λ to develop a new rainfall-runoff prediction model.

Table 1. Inferential statistics results of derived λ for M70 decadal dataset at α = 0.01.

λ	Statistics	Bootstrap, BCa 99%			
		Bias	Std. Error	Confidence Intervals Lower	Upper
Skewness	3.815				
Kurtosis	19.768				
Mean	0.098	0.0003	0.014	0.069	0.142
Median	0.065	0.0006	0.00294	0.049	0.089

Table 2. Inferential statistics results of derived λ for M80 decadal dataset at α = 0.01.

λ	Statistics	Bootstrap, BCa 99%			
		Bias	Std. Error	Confidence Intervals Lower	Upper
Skewness	3.217				
Kurtosis	13.028				
Mean	0.095	0.0002	0.014	0.066	0.135
Median	0.047	0.0022	0.007	0.034	0.064

Table 3. Inferential statistics results of derived λ for M90 decadal dataset at α = 0.01.

λ	Statistics	Bootstrap, BCa 99%			
		Bias	Std. Error	Confidence Intervals Lower	Upper
Skewness	5.393				
Kurtosis	34.674				
Mean	0.076	0.00005	0.013	0.051	0.115
Median	0.042	0.00183	0.007	0.031	0.063

The λ dataset is skewed and tested to be non-normally distributed in SPSS for all three decadal groups and therefore, the search for an optimal representative λ value using a supervised optimization technique will be concentrated on the range of median confidence intervals. These intervals are [0.049, 0.089] for the M70 dataset (Table 1), [0.034, 0.064] for the M80 dataset (Table 2), and [0.031, 0.063] for the M90 dataset (Table 3).

The BCa 99% confidence intervals of S_λ for the M70, M80, and M90 decadal datasets are presented in Tables 4–6. The normality of the S_λ dataset was tested using SPSS for all three decadal groups, and found to be normally distributed. Therefore, the optimal S_λ value was searched for within the range of the mean confidence intervals. There intervals are [117.083, 187.008] for M70 dataset (Table 4), [141.892, 231.088] for M80 dataset (Table 5), and [131.989, 192.939] for M90 dataset (Table 6).

Table 4. Inferential statistics results of derived S_λ for M70 decadal dataset at $\alpha = 0.01$.

S_λ	Statistics	Bootstrap, BCa 99%			
		Bias	Std. Error	Confidence Intervals	
				Lower	Upper
Skewness	1.298				
Kurtosis	0.975				
Mean	151.592	−0.482	14.954	117.083	187.008
Median	123.615	−0.166	11.367	91.255	157.815

Table 5. Inferential statistics results of derived S_λ for M80 decadal dataset at $\alpha = 0.01$.

S_λ	Statistics	Bootstrap, BCa 99%			
		Bias	Std. Error	Confidence Intervals	
				Lower	Upper
Skewness	1.794				
Kurtosis	5.201				
Mean	180.994	−0.339	14.954	141.892	231.088
Median	147.950	−3.921	19.112	113.890	183.670

Table 6. Inferential statistics results of derived S_λ for M90 decadal dataset at $\alpha = 0.01$.

S_λ	Statistics	Bootstrap, BCa 99%			
		Bias	Std. Error	Confidence Intervals	
				Lower	Upper
Skewness	1.132				
Kurtosis	1.407				
Mean	161.827	0.221	11.934	131.989	192.939
Median	142.610	−2.566	21.298	95.236	189.506

The optimal λ and S_λ values for the M70, M80, and M90 decadal datasets using a supervised optimization technique are presented in Table 7. The product of the optimal λ and S_λ values gives the representative initial abstraction value for each dataset, which can be calculated as $I_a = \lambda S_\lambda$.

Table 7. Optimal λ, S_λ and I_a for M70, M80 and M90 decadal datasets.

Dataset	Optimal λ	Optimal S_λ	$I_a = \lambda S_\lambda$
M70	0.049	160 mm	7.904 mm
M80	0.034	190 mm	6.431 mm
M90	0.031	160 mm	4.956 mm

3.2. The Decadal Rainfall-Runoff Models

The decadal rainfall-runoff models for Peninsula Malaysia are presented in Table 8 by substituting the respective I_a and S_λ values from Table 7 into Equation (1). Equations (3)–(5) were then formulated to model the decadal rainfall-runoff conditions in Peninsula Malaysia. To further analyse decadal runoff trend across multiple rainfall depths and $CN_{0.2}$ scenarios in Peninsula Malaysia, Equations (3)–(5) need to be re-expressed in terms of $CN_{0.2}$ to benefit SCS practitioners as they are more familiar with the use of curve number [50].

Table 8. Decadal rainfall-runoff models for M70, M80 and M90 decadal datasets.

Dataset	Runoff Predictive Model	Nash-Sutcliffe Index	Equation Number
M70	$Q = \frac{(P-7.904)^2}{P-152.096}$	0.958	(3)
M80	$Q = \frac{(P-6.431)^2}{P-183.569}$	0.910	(4)
M90	$Q = \frac{(P-4.956)^2}{P-155.044}$	0.907	(5)

Q = runoff depth (mm), P = rainfall depth (mm).

To calculate S_λ and $S_{0.2}$ for each decadal dataset, the general S_λ formula (step 8 in methodology Section 2.2) can be used with the optimum λ values. Through SPSS, this study identified statistically significant power function correlation between S_λ and $S_{0.2}$ for the M70, M80, and M90 decadal datasets, which is consistent with previous research findings [66–68]. The final equations are listed in Table 9.

Table 9. Correlation equations between S_λ and $S_{0.2}$ for M70, M80 and M90 decadal datasets.

Dataset	Correlation Equation	Adjusted R-Squared	Standard Error of Estimate	Equation Number
M70	$S_{0.049} = 1.184{S_{0.2}}^{1.081}$	0.939	0.134	(6)
M80	$S_{0.034} = 1.107{S_{0.2}}^{1.094}$	0.910	0.201	(7)
M90	$S_{0.031} = 1.179{S_{0.2}}^{1.069}$	0.907	0.165	(8)

All correlations are significant at $p < 0.001$.

Equations (6)–(8) played a crucial role in converting S_λ to $S_{0.2}$, enabling SCS practitioners to use a rainfall-runoff model with $CN_{0.2}$, which they are more familiar with. Furthermore, by establishing a correlation between the newly derived S_λ and $S_{0.2}$, Equations (3)–(5) were modified to be expressed in $CN_{0.2}$ terms, facilitating decadal trend analyses with $CN_{0.2}$.

Equations (3)–(5) can be expressed in $CN_{0.2}$ by substituting S_λ in Equation (1) with Equations (6)–(8), as well as the SCS-CN formula (Step 10 in methodology Section 2.2). By doing so, the decadal runoff predictive models can be re-expressed as shown in Appendix B. The resulting alternate representations for decadal runoff predictive models in Peninsula Malaysia are presented in Table 10 in term of $CN_{0.2}$.

Table 10. Alternate form of decadal rainfall-runoff models for M70, M80 and M90 decadal datasets.

Dataset	Runoff Predictive Model	Equation Number
M70	$Q_{0.049} = \frac{\left[P-23.077\left(\frac{100}{CN_{0.2}}-1\right)^{1.081}\right]^2}{\left[P+447.876\left(\frac{100}{CN_{0.2}}-1\right)^{1.081}\right]}$	(9)
M80	$Q_{0.034} = \frac{\left[P-15.992\left(\frac{100}{CN_{0.2}}-1\right)^{1.094}\right]^2}{\left[P+456.589\left(\frac{100}{CN_{0.2}}-1\right)^{1.094}\right]}$	(10)
M90	$Q_{0.031} = \frac{\left[P-13.618\left(\frac{100}{CN_{0.2}}-1\right)^{1.069}\right]^2}{\left[P+425.963\left(\frac{100}{CN_{0.2}}-1\right)^{1.069}\right]}$	(11)

3.3. The Decadal Runoff Trend Analyses

The decadal runoff models (Equations (9)–(11)) enable the quantification of runoff conditions for various decades under different rainfall depths (P) and $CN_{0.2}$ scenarios, facilitating the analysis of runoff changes. The DID HP 27 dataset contains the lowest and highest recorded rainfall depths, ranging from 20 mm to 430 mm across $CN_{0.2}$ classes from 46 to 94. Runoff difference tables can then be calculated between any two decadal models.

This study evaluated the inter-decadal runoff differences between M70 and M80, M80 and M90, and M70 and M90 in Peninsula Malaysia. The runoff amount of the earlier

decade was subtracted from the latter to determine the inter-decadal runoff difference. For instance, the inter-decadal runoff difference between M70 (Equation (9)) and M80 (Equation (10)) was calculated by subtracting the runoff amount of M70 from that of M80. A positive inter-decadal runoff difference amount indicated a larger runoff amount in M80 compared to M70 and vice versa. Statistical analyses were performed to determine significant runoff trends between different decades. This study also correlated decadal runoff changes with deforestation and urbanization data in Peninsula Malaysia.

Non-parametric Kendall's Tau b and Spearman's Rho statistics were used to evaluate the inter-decadal runoff trend in SPSS. Both statistics showed a significant positive correlation (2-tailed) at alpha = 0.01 for all inter-decadal periods, rainfall depths, and $CN_{0.2}$ classes mentioned above. This positive correlation indicates an upward trend in inter-decadal runoff, which can be visually represented in Figures 1–3. To assess the magnitude of this upward trend in each inter-decadal scenario and $CN_{0.2}$ class (ranging from 46 to 94) according to rainfall depths from 20 mm to 430 mm, Sen slopes and its collective inferential statistics were calculated. The Sen slopes and inferential statistics of all $CN_{0.2}$ classes were then analysed collectively for each inter-decadal scenario at the alpha = 0.01 level, and the results are tabulated in Tables 11–13.

Table 11. Inferential statistics of Sen Slopes for inter decadal runoff difference between M80 and M90.

Sen Slopes M80 to M90	Statistics	Bootstrap, BCa 99%			
		Bias	Std. Error	Confidence Intervals Lower	Upper
Skewness	−0.022				
Kurtosis	−1.512				
Mean	0.0121	−0.00002	0.00225	0.00701	0.01720
Median	0.0127	−0.00029	0.00422	0.00439	0.02119
Std. Deviation	0.0087	−0.00039	0.00103	0.00588	0.01032
Range	0.0247				

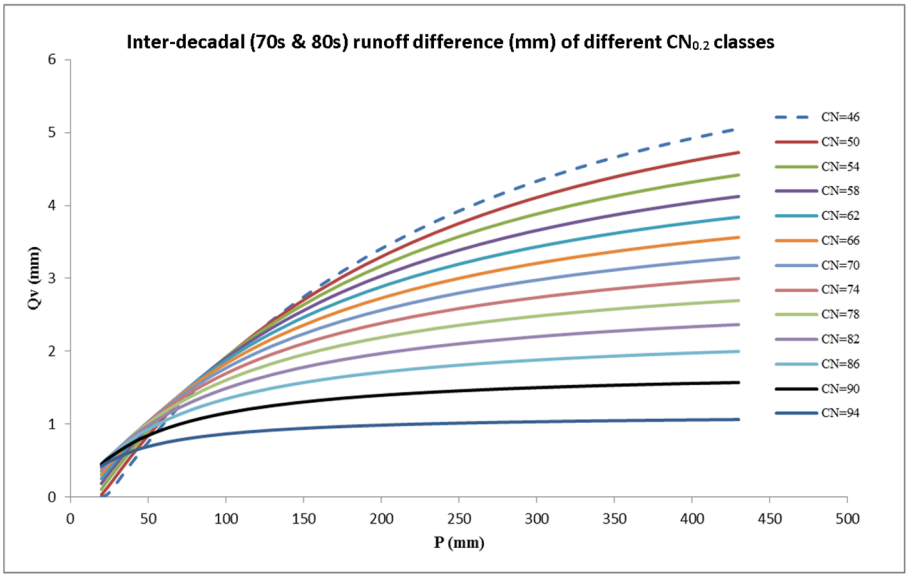

Figure 1. Decadal runoff difference of Equations (9) and (10) for selected $CN_{0.2}$ values to reflect the runoff change between M70 and M80 under different rainfall depths.

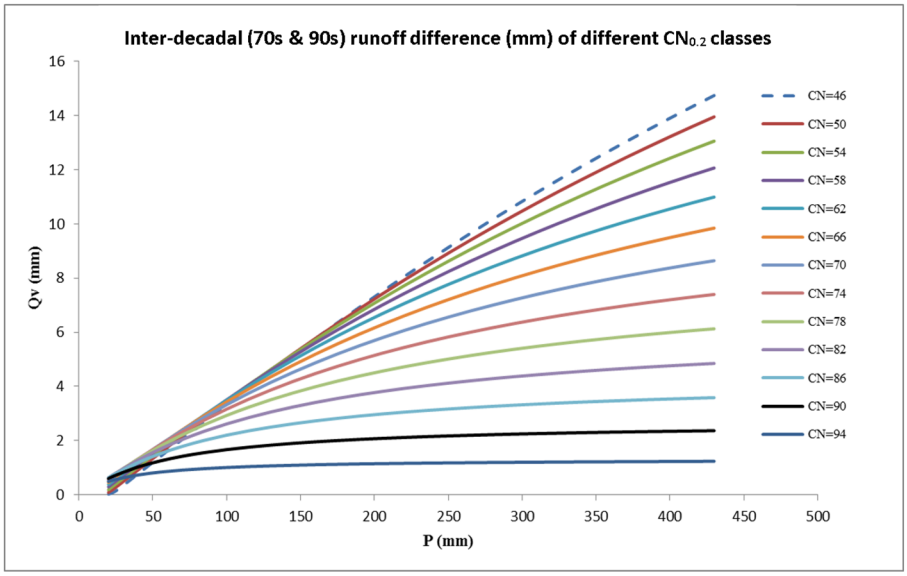

Figure 2. Decadal runoff difference of Equations (9) and (11) for selected $CN_{0.2}$ values to reflect the runoff change between M70 and M90 under different rainfall depths.

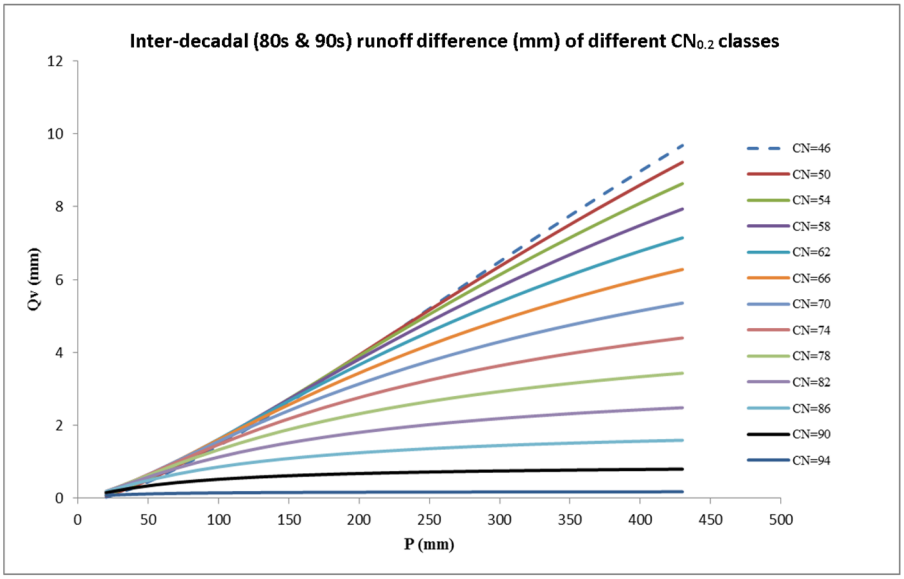

Figure 3. Decadal runoff difference of Equations (10) and (11) for selected $CN_{0.2}$ values to reflect the runoff change between M80 and M90 under different rainfall depths.

Table 12. Inferential statistics of Sen Slopes for inter decadal runoff difference between M70 and M80.

Sen Slopes M70 to M80	Statistics	Bootstrap, BCa 99%			
		Bias	Std. Error	Confidence Intervals Lower	Upper
Skewness	0.272				
Kurtosis	−0.940				
Mean	0.0051	−0.00001	0.00081	0.00313	0.00713
Median	0.0048	0.00008	0.00126	0.00230	0.00824
Std. Deviation	0.0031	−0.00015	0.00046	0.00178	0.00396
Range	0.1000				

Table 13. Inferential statistics of Sen Slopes for inter decadal runoff difference between M70 and M90.

Sen Slopes M70 to M90	Statistics	Bootstrap, BCa 99%			
		Bias	Std. Error	Confidence Intervals Lower	Upper
Skewness	0.065				
Kurtosis	−1.473				
Mean	0.0178	−0.00003	0.00322	0.01049	0.02506
Median	0.0175	0.00015	0.00589	0.00712	0.03125
Std. Deviation	0.0124	−0.00057	0.00149	0.00823	0.01479
Range	0.0353				

Calculated Sen slope values were tested as normally distributed in SPSS. Therefore, the mean Sen slope value was used to represent each inter-decadal runoff scenario. On average, the collective Sen slope value was 0.0121 (p = 0.01, 99% confidence interval from 0.00701 to 0.01720) to indicate the runoff incremental trend between M80 and M90. The Sen slope between M70 and M80 was 0.0051 (p = 0.01, 99% confidence interval from 0.00313 to 0.00713), while between M70 and M90 it was 0.0178 (p = 0.01, 99% confidence interval from 0.01049 to 0.02506). The Sen slope values also estimated the percentage of rainfall depth that becomes incremental runoff. For instance, the average expected runoff increment from a rainfall depth of 100 mm across $CN_{0.2}$ classes from 46 to 94 can be estimated to be 1.21 mm between M80 and M90 (i.e., 0.0121 × 100 mm).

The study conducted a repetition of all statistical analyses with a $CN_{0.2}$ range of 46 to 70 to assess the runoff changes across lower $CN_{0.2}$ classes, which correspond to rural and forested catchments. This was done to obtain a more accurate estimate of the inter-decadal runoff increment conditions in these areas. The results showed that the runoff incremental trend between M80 and M90 of $CN_{0.2}$ (46 to 70) had a Sen slope value of 0.0190 (p = 0.01, 99% confidence interval from 0.01595 to 0.02216). The Sen slope value between M70 and M80 was 0.0075 (p = 0.01, 99% confidence interval from 0.00606 to 0.00898), and between M70 and M90, it was 0.0276 (p = 0.01, 99% confidence interval from 0.02262 to 0.03239). For example, the expected runoff increment from rainfall of 100 mm across $CN_{0.2}$ classes from 46 to 70 was estimated to be 1.90 mm between M80 and M90. The study found that runoff increments were significant (p = 0.01) between all inter-decadal scenarios and were more apparent in forested and rural areas (highlighted area in Figure 4).

Positive inter-decadal runoff difference in Peninsula Malaysia is depicted in Figures 1–3. High rainfall depths and low $CN_{0.2}$ groups, which are associated with forested catchments, are particularly affected. These study outcomes are in line with previous studies [67–70]. Inter-decadal runoff differences are more pronounced under high rainfall depths. The mean runoff of different decades across different $CN_{0.2}$ classes was calculated and compiled, as shown in Figure 5. M90 had the highest runoff, while M70 had the lowest. Greater percentage changes in mean runoff were observed in lower $CN_{0.2}$ classes (forested catchments) compared to higher $CN_{0.2}$ classes (urban area). The largest mean runoff incremental percentage was 12.6% (6.6 mm) from M70 to M90 at $CN_{0.2}$ = 46, while the smallest change was 0.1% (0.1 mm) from M80 to M90 at $CN_{0.2}$ = 94.

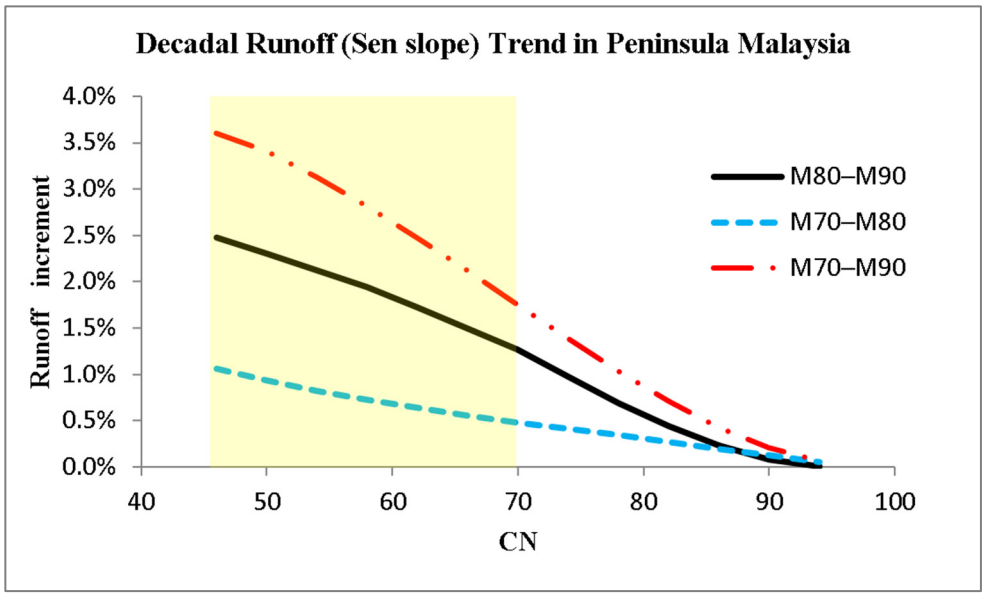

Figure 4. The Sen Slope for decadal runoff increment for $CN_{0.2}$ classes between M70 to M90. Sen slopes and inferential statistics were used to analyse the collective inter-decadal runoff increment conditions. Forested and rural areas are highlighted at lower $CN_{0.2}$ area from 46 to 70. The estimated percentage of rainfall depths by Sen slope calculation were compared between all scenarios to contrast the inter-decadal runoff incremental percentage.

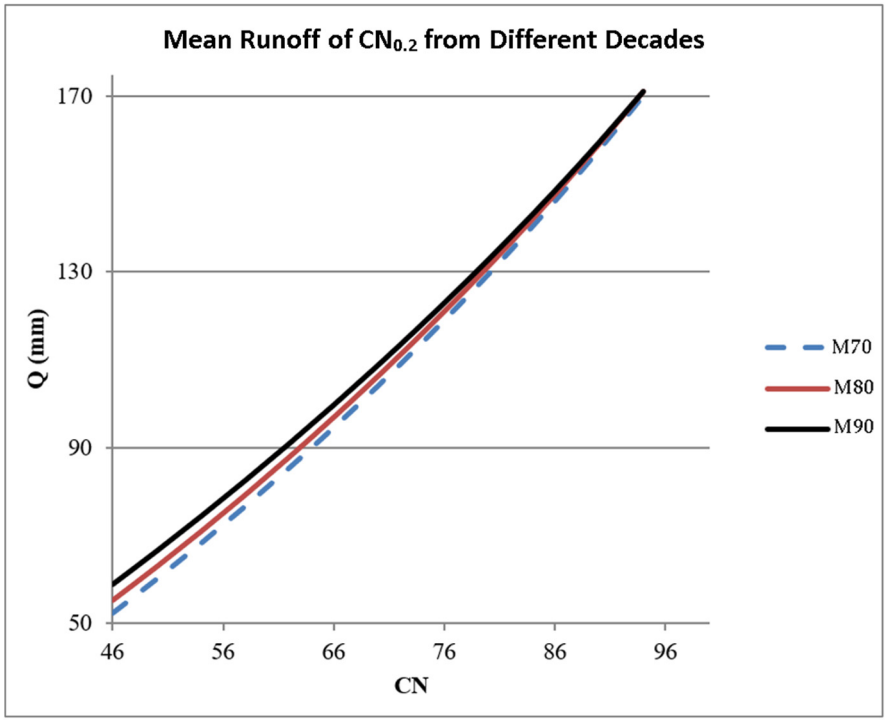

Figure 5. Mean runoff (mm) of decadal datasets of M70, M80, and M90 for selected $CN_{0.2}$ values.

3.4. The Impact of $CN_{0.2}$ Variation on Runoff

According to [71], due to variation in hydrological conditions, $CN_{0.2}$ value is often calibrated to match observed runoff dataset in modelling practice. Researchers observed that a variation of ±10% in $CN_{0.2}$ might lead to ±50% runoff variation [72] while [73] it was reported that even 1% increase in $CN_{0.2}$ with rainfall depth of 175 mm had caused 2.03% increase in runoff. References [73,74] concluded that $CN_{0.2}$ variations will have a larger impact on runoff than other parameters in Equation (1).

$CN_{0.2}$ tweaking becomes a convenient way to calibrate and validate hydrological models. However, other studies reported that $CN_{0.2}$ value of a catchment was unstable and decreased when rainfall increased [74–76]. The error and sensitivity analysis results by some researchers stated that $CN_{0.2}$ variations would induce a larger impact on runoff calculation with inherent error rather than rainfall depth variations [72,74,77]. $CN_{0.2}$ tweaking might achieve or improve temporal hydrological modelling accuracy through the trial-and-error technique, but the practicality of the end result was often uncertain and lack of statistical justification.

This study modelled the impact of $CN_{0.2}$ variation with the DID HP 27 dataset. According to [78], the practical CN values were likely to be within the range of 40 to 98. The optimum best collective $CN_{0.2}$ was 71 for the entire DID HP 27 dataset, thus, $CN_{0.2}$ variation up to 40% was chosen to cover the range of $CN_{0.2}$ from 43 to 99 and rainfall from 20 mm to 430 mm. $CN_{0.2}$ upscaling induced larger runoff change than downscaling while both effects were largely felt at rainfall depths below 100 mm. On average, runoff would reduce by 37% when $CN_{0.2}$ was downscaled up to 40% between 20 mm and 430 mm. On the other hand, the average runoff increased by 306% when $CN_{0.2}$ was upscaled up to 40%. The average runoff for both scenarios was almost identical when rainfall depths were limited to higher rainfall depths (100 mm to 430 mm). The average runoff reduced by 34% when $CN_{0.2}$ was downscaled up to 40%, while average runoff increased by 35% when $CN_{0.2}$ was upscaled to the same range. Varying the $CN_{0.2}$ value by ±10% resulted in an average runoff change of 40%, which is consistent with the findings reported in [72]. Similarly, upscaling the $CN_{0.2}$ value by 1% with a rainfall depth of 175 mm caused a 2% increase in runoff, which matches the range reported by [73]. Sen slope analyses showed that in both $CN_{0.2}$ upscaling and downscaling scenario, runoff reduction and incremental rates reduced toward the high rainfall depths but increased according to the $CN_{0.2}$ variation percentage. Lower rainfall depths (20 to 100 mm) had higher runoff variation percentages than higher rainfall depths (100 to 430 mm), as reported by previous studies [67–70]. Figures 6 and 7 present the overview of the impact of $CN_{0.2}$ variation on runoff with equations to estimate the percentage change in runoff.

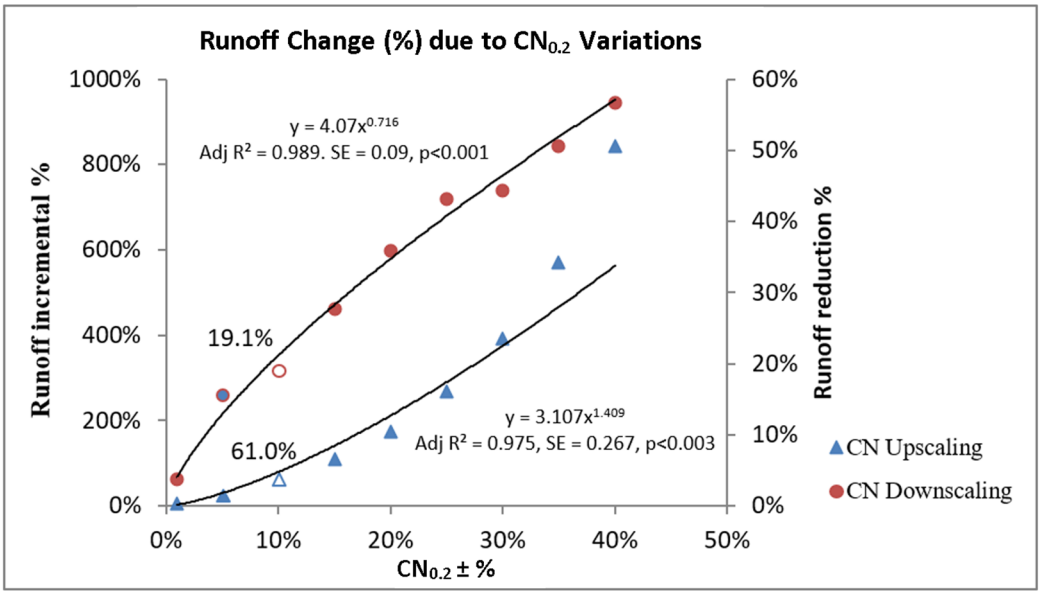

Figure 6. Effects of upscaling and downscaling of $CN_{0.2}$ on runoff. $CN_{0.2}$ upscaling caused runoff incremental change and vice versa. Note: $CN_{0.2}$ upscaling data points refer to primary axis. $CN_{0.2}$ variations start from $CN_{0.2}$ = 71, variation range (43 to 99) across rainfall depth range from 25 mm to 425 mm. The blank circle and triangular data point are benchmark points of $CN_{0.2}$ ± 10%, the indicated 19.1% and 61% are runoff reduction and incremental due to $CN_{0.2}$ variations.

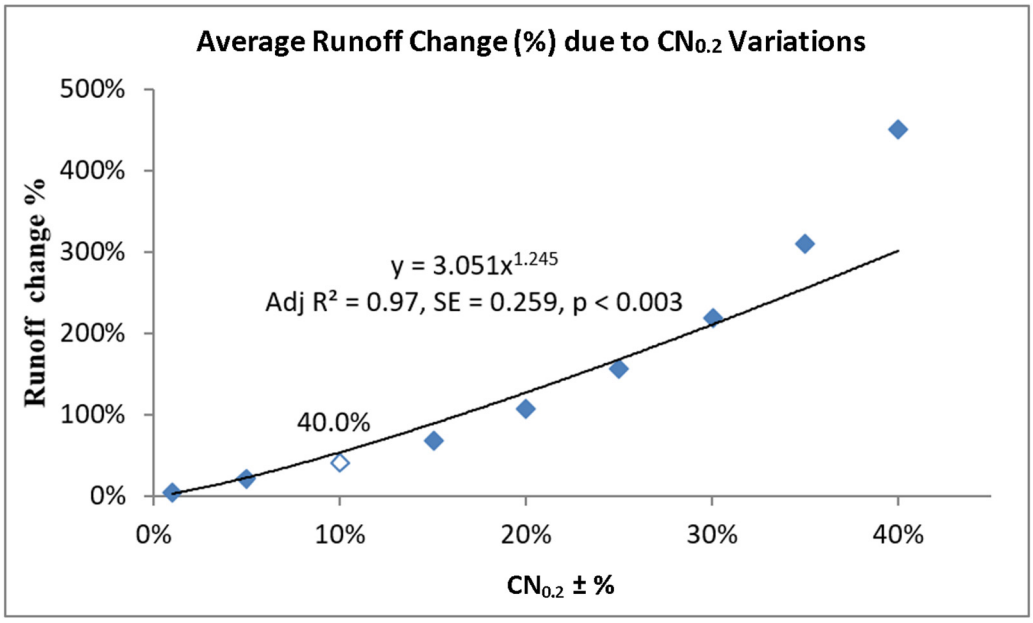

Figure 7. Response of runoff change to variation of $CN_{0.2}$. Runoff change % data points are the averaged runoff change due to $CN_{0.2}$ upscaling and downscaling of a specific variation %. The blank data point shows the average runoff change % due to $CN_{0.2}$ ± 10% variation.

3.5. The Impact of Deforestation and Urbanization on Runoff in Peninsula Malaysia

According to statistics from the Malaysia Department of Forestry, Peninsula Malaysia went through extensive deforestation from the 1970s. Forest area decreased at fast rates in the 1980s and started to stabilise in the 1990s. Forest area had reduced by 21.1% from M70 to M80 and 25.5% from M70 to M90 (Figure 8). Figure 9 was created to show the relationship between these decadal forest area reduction rate and its corresponding mean inter-decadal incremental runoff difference (Q_v%) across different $CN_{0.2}$ classes in Peninsula Malaysia. During the period between M70 and M90 in Peninsula Malaysia, the mean excess (incremental) runoff volume difference for $CN_{0.2}$ classes ranging from 46 to 70 was calculated to be 6.8 mm, equivalent to 6.8 million litres per square kilometre. This corresponds to a 10.2% increase in excess runoff, and it occurred simultaneously with a 25.5% decrease in forest area. These findings provide insights into the hydrological impacts of deforestation on non-homogeneous catchments. In general, inter-decadal mean runoff differences were more pronounced in forested and rural catchments (lower $CN_{0.2}$ classes) than urban areas. Inter-decadal runoff difference between M70 and M90 is significantly greater than runoff difference between M70 and M80 (Figure 9).

According to the published data and figures from the Department of Statistics Malaysia [79–87], the urban population in Peninsula Malaysia had been increasing rapidly (Table 14). In comparison to the forest area statistics from the Department of Forestry [53–59], an inverse correlation was identified in SPSS as:

$$FA = 5.533 + (4.922/Urb\text{-}pop) \quad (12)$$

$R^2_{adj} = 0.964$, SE = 0.175, $p < 0.012$
FA = Forest area (Million hectare)
Urb-pop = Urban population in Peninsula Malaysia (Millions)

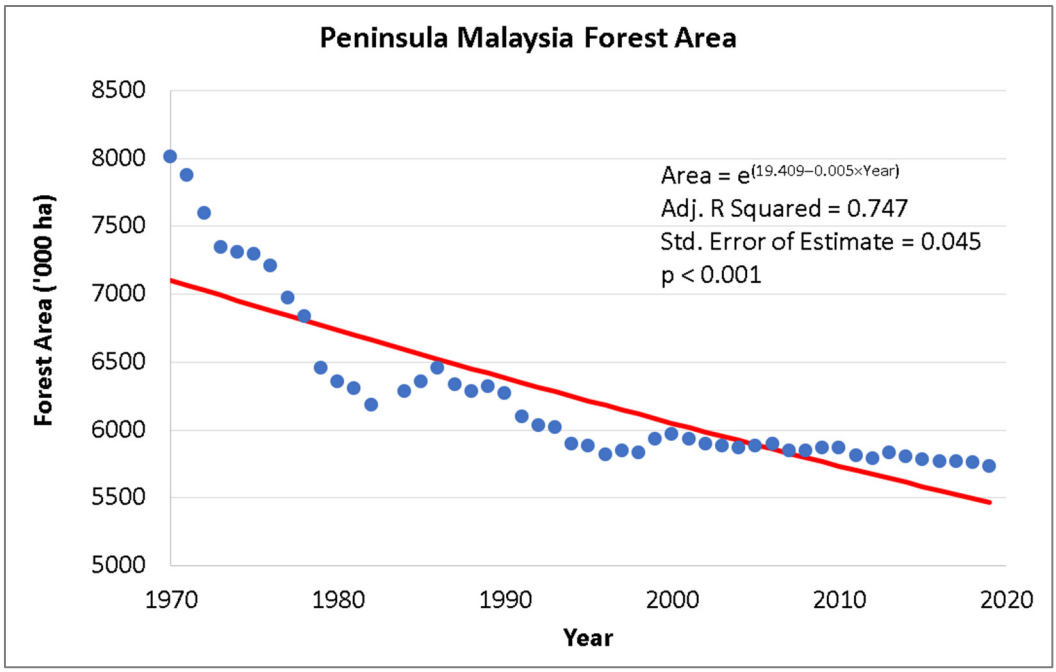

Figure 8. Annual statistics of forest area in Peninsula Malaysia [12,53–59,79].

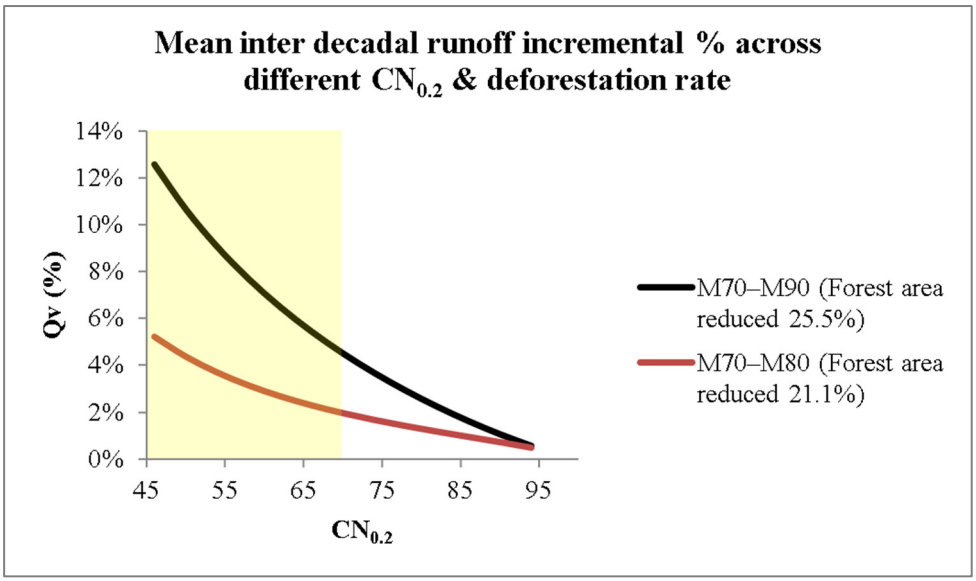

Figure 9. Mean inter-decadal runoff incremental % across different $CN_{0.2}$ classes (46 to 70) between 1970 (M70) and 2000 (M90). Note: The graph was created with decadal runoff models and Malaysia Department of Forestry data to coincide with the total forest area loss within the same period. On average, runoff volume for $CN_{0.2}$ classes ranging from 46 to 70 increased by 10.2% in Peninsular Malaysia while forest area reduced by 25.5% from 1970 to 2000.

The inverse correlation between urban population and the forest area in Peninsula Malaysia implies that urban development has significant correlations with deforestation (Figure 8). On the other hand, the deforestation has a direct impact on runoff amount as shown in Figure 9.

Table 14. Decadal urban population and forest area in Peninsula Malaysia [12,80–87].

Year	Urban Population (Millions)	Forest Area (Millions Hectare)
1970	2.03	8.01
1980	4.81	6.35
1990	7.97	6.27
2000	12.26	5.97

3.6. Decadal λ and I_a

In recent decades, urbanization in Peninsula Malaysia has caused uneven land development, leading to non-homogeneity in catchments. This study aimed to address this issue by calibrating the SCS-CN model using rainfall-runoff data from different decades to develop decadal models. The models demonstrated a strong ability to estimate runoff amounts, achieving a Nash-Sutcliffe Index ranging from 0.907 to 0.958 (Table 8), even in non-homogeneous catchments. These findings suggest that recalibrating the SCS-CN models based on regional and decadal specific rainfall-runoff conditions could be an effective approach for estimating runoff in non-homogeneous catchments.

In a previous study by the authors, the optimum λ value for the entire DID HP 27 dataset was identified as 0.051 to model overall runoff conditions. However, in this study, different optimum λ values were derived for the decadal datasets of M70, M80, and M90, which also led to changes in the corresponding initial abstraction (I_a) values (Table 7). Over time, the optimal λ and I_a values for each decade were found to decrease, indicating changes in land cover resulting from deforestation and urbanization that impact runoff conditions in rural catchments. The decreasing trend in λ leads to a corresponding increase in runoff over time in Peninsula Malaysia.

SCS practitioners commonly calibrate $CN_{0.2}$ with one batch of runoff data and validate the final results against another batch to determine the optimum $CN_{0.2}$ value for modelling a combined dataset. However, this study highlights concerns with this practice due to land-use and land-cover changes in Peninsula Malaysia, which directly affect catchment runoff conditions over time.

There is a statistically significant upward trend in runoff (at alpha = 0.01) across all $CN_{0.2}$ classes from M70 to M90 due to changes in land use. Therefore, SCS practitioners must be cautious and aware that blindly accepting the λ value as 0.2 is not advisable, and it is strongly recommended to derive a regional-specific λ value. Although an optimum λ value of 0.051 was used in a previous study [50] to model the entire dataset with a Nash-Sutcliffe value of 0.92, it differed significantly from the optimum λ values of different decades. Hence, runoff predictive models formulated with different optimum λ values will yield differences in runoff predictions.

3.7. Rainfall Trend Analyses

The BCa bootstrapping method with a 99% confidence interval was used to analyse the monthly rainfall trend in Peninsula Malaysia (Figure 10), which revealed that there has been no significant trend in the monthly rainfall over the past 20 years. The forecasted rainfall from 2021 to 2022 was consistent with the current trend. The results were supported by the model generated by Expert Modeler (Figure 11), which indicated that there would be no significant alteration in the rainfall trend in the near future.

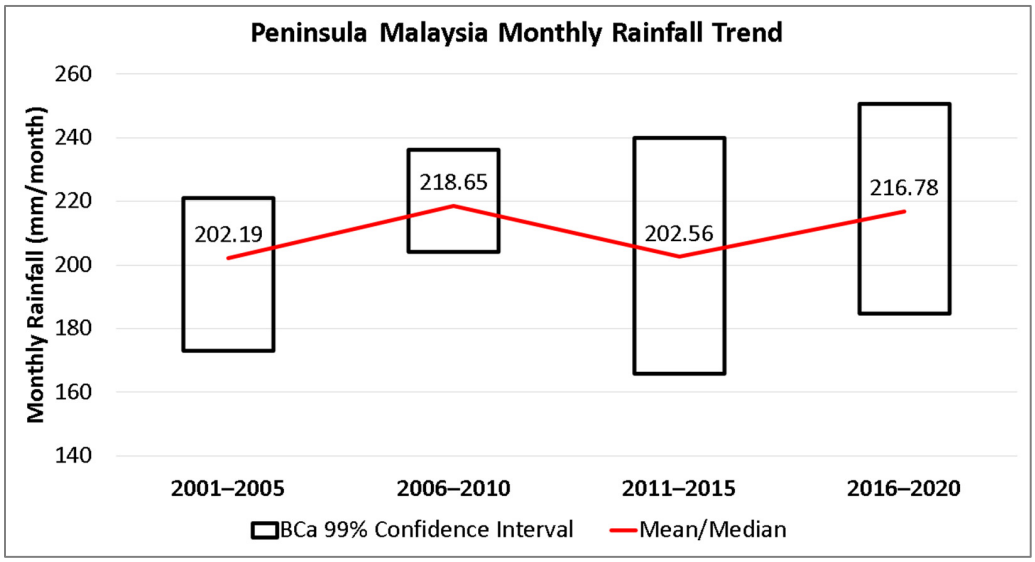

Figure 10. Monthly rainfall trend in Peninsula Malaysia from 2001 to 2020 (divided into 5-year interval).

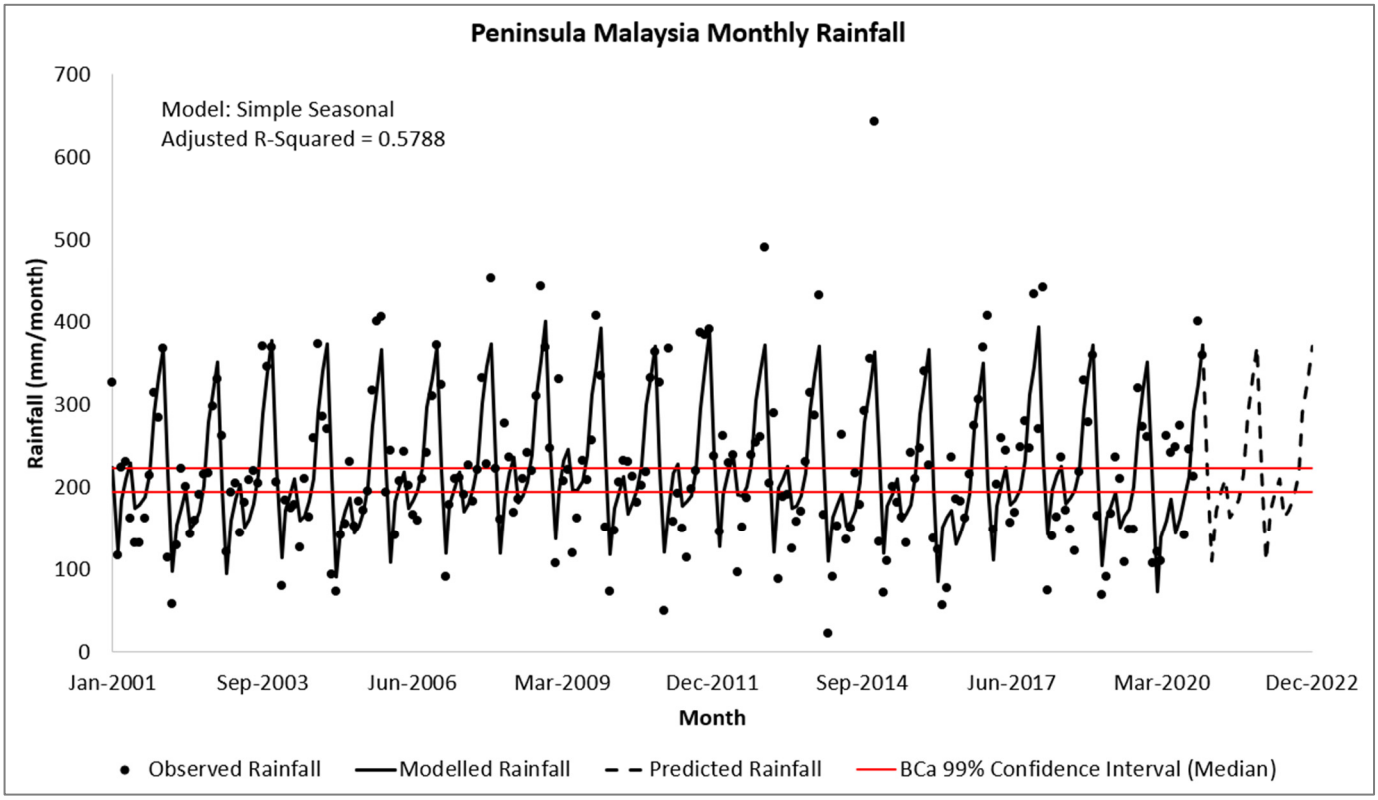

Figure 11. Monthly rainfall time series forecasting model for Peninsula Malaysia using Expert Modeler. Modelled period: 2001–2020 (N = 240, see Appendix A). Forecasted period: 2021–2022 (N = 24).

Flood occurrences are strongly influenced by changes in land use, including deforestation, agricultural activities, and urbanization. The conversion of natural land cover to urban and other developed land use can significantly alter the hydrological cycle, resulting in increased surface runoff and reduced infiltration. This alteration of the landscape can lead to changes in the frequency, magnitude, and timing of floods, as well as increased erosion and sedimentation in rivers and streams [37].

The increase in surface runoff resulting from the conversion of natural land for human use has caused major flooding in Malaysia [88]. Floods are the most destructive natural disasters in the country, with an estimated 85 river basins, mainly in Peninsula Malaysia, prone to recurrent flooding. Based on a study in 2014, approximately 9% of the total area of Malaysia, covering 29,800 km^2, is vulnerable to flood disaster, affecting almost 4.82 million people, equivalent to 22% of the total population [89]. In 2014, the states of Johor, Kelantan, Pahang, Perak, and Terengganu in Peninsula Malaysia, which were severely affected by floods, also recorded high rates of forest loss [38].

Recent floods and landslides in Malaysia have been attributed to deforestation, which results in the release of sediment and weakened soil. Trees help to prevent sediment runoffs and hold water, making them an essential factor in maintaining a stable environment. The excessive clear-cutting of trees for oil palm plantations has been identified as the primary cause of mudslides in recent times, with poor construction standards also contributing to the problem. Therefore, it can be inferred that deforestation and poor construction standards are the key factors responsible for these events, rather than El Niño or global warming, as suggested by studies [90–94].

4. Conclusions

This study adopted the CN hydrological model calibration technique developed by the authors in a previous study [50] and applied it in decadal runoff prediction study in Peninsula Malaysia. The correlation between forest area reduction, urbanization, and runoff volume increment was established. Highlights of the study are summarized as below:

1. The use of the conventional SCS-CN runoff model will commit type II error in this study to predict runoff conditions of different study periods. It must be pre-justified with statistics and calibrated prior to adoption for any runoff prediction. It is also not recommended to conduct calibration and validation on the entire DID HP 27 dataset of this study as each demarcated decade was represented with its unique and statistically significant runoff predictive model. Calibration and validation methodology based on the conventional SCS-CN runoff model fail to quantify accurate runoff conditions spanning across different time periods with significant land-use and cover change.
2. CN adjustment practice to formulate a hydrological model can have a large inherent error as small adjustments on the curve number can lead to large variation in the runoff. Given sufficient sample size, SCS-CN runoff model should be calibrated and formulated according to its unique optimum λ values to represent rainfall-runoff conditions of different time periods. In this study, when CN value was varied $\pm$ 10%, the average runoff changed by 40%. This study found a significant increase in runoff across all $CN_{0.2}$ classes in Peninsula Malaysia due to changes in land use, emphasizing the importance of deriving a regional-specific λ value and cautioning that different optimum λ values for different decades will yield differences in runoff predictions.
3. This study emphasizes the significance of accounting for regional and decadal-specific rainfall-runoff conditions to estimate runoff in non-homogeneous catchments effectively. The calibrated SCS-CN model using data from different decades showed a remarkable ability to accurately estimate runoff amounts, even in non-homogeneous catchments. The models achieved a strong ability to estimate runoff amounts, attaining a Nash-Sutcliffe Index ranging from 0.907 to 0.958, even in non-homogeneous catchments.
4. Calibrated SCS decadal (lump) runoff models show significant decadal runoff uptrend which coincides with the overall deforestation rate in Peninsula Malaysia. The presented methodology may become more apparent with regional specific deforestation rate and its corresponding rainfall-runoff dataset. The reduction of forest area by 25.5% in Peninsula Malaysia between 1970 and 2000 was found to be directly proportional to an increase in excess runoff volume of 10.2%. In general, inter-decadal mean

runoff differences were more pronounced in forested and rural catchments (lower CN classes) than urban areas.

5. NASA's Giovanni system was used to generate 20 years of annual rainfall maps while monthly rainfall data (2001 to 2020) was also extracted for trend analysis and short-term forecast. This study found no significant uptrend in the rainfall within the period, and the occurrence of flood and landslide incidents can likely be attributed to land-use changes in Peninsula Malaysia.

Author Contributions: Conceptualization, L.L.; methodology, J.F.K. and L.L.; software, J.F.K. and L.L.; validation, S.L. and L.L.; formal analysis, J.F.K. and L.L.; investigation, J.F.K. and L.L.; resources, J.F.K. and L.L.; data curation, J.F.K. and L.L.; writing—original draft preparation, J.F.K. and L.L.; writing—review and editing, J.F.K., S.L., V.L.L. and L.L; visualization, J.F.K. and L.L.; supervision, L.L.; project administration, L.L.; funding acquisition, L.L. All authors have read and agreed to the published version of the manuscript.

Funding: This research was supported by the Ministry of Higher Education (MoHE) through the Fundamental Research Grant Scheme (FRGS/1/2021/WAB07/UTAR/02/1) and partly supported by the Brunsfield Engineering Sdn. Bhd., Malaysia industrial grants (Brunsfield 8013/0002 & 8126/0001).

Data Availability Statement: Rainfall-runoff data is available at the appendix of DID, Hydrological Procedure No. 27. Design Flood Hydrograph Estimation for Rural Catchments in Peninsula Malaysia. JPS, DID, Kuala Lumpur. 2010. Available online: https://www.water.gov.my/jps/resources/PDF/Hydrology%20Publication/Hydrological_Procedure_No_27_(HP_27).pdf (accessed on 10 March 2023). IMERG-F monthly version 6 product at a spatial resolution of 0.1° data can be obtained from the NASA's Giovanni system (https://giovanni.gsfc.nasa.gov/giovanni (accessed on 15 October 2021)). Authors would like to thank Zhen Xiang Soo (Eugene) for sharing the IMERG-F data with us.

Conflicts of Interest: The authors declare no conflict of interest.

Appendix A

Table A1. Monthly rainfall in Peninsula Malaysia from 2001 to 2009 [64].

Year	Month	Rainfall (mm/Month)	Year	Month	Rainfall (mm/Month)	Year	Month	Rainfall (mm/Month)
2001	1	326	2004	1	206	2007	1	323
	2	117		2	80		2	92
	3	224		3	185		3	179
	4	231		4	174		4	210
	5	162		5	178		5	211
	6	132		6	127		6	191
	7	132		7	211		7	226
	8	163		8	163		8	183
	9	214		9	259		9	221
	10	314		10	374		10	332
	11	285		11	285		11	229
	12	367		12	270		12	452
2002	1	114	2005	1	94	2008	1	223
	2	58		2	73		2	160
	3	129		3	142		3	278
	4	223		4	155		4	236
	5	200		5	230		5	169
	6	144		6	152		6	185
	7	159		7	183		7	210
	8	191		8	172		8	242
	9	216		9	195		9	220
	10	217		10	318		10	310
	11	298		11	401		11	443
	12	330		12	406		12	370

Table A1. *Cont.*

Year	Month	Rainfall (mm/Month)	Year	Month	Rainfall (mm/Month)	Year	Month	Rainfall (mm/Month)
2003	1	263	2006	1	194	2009	1	248
	2	122		2	244		2	107
	3	193		3	142		3	330
	4	204		4	208		4	208
	5	14		5	243		5	221
	6	181		6	201		6	120
	7	209		7	167		7	162
	8	220		8	160		8	232
	9	205		9	210		9	209
	10	370		10	242		10	257
	11	345		11	310		11	407
	12	369		12	372		12	335

Table A2. Monthly rainfall in Peninsula Malaysia from 2010 to 2018 [64].

Year	Month	Rainfall (mm/Month)	Year	Month	Rainfall (mm/Month)	Year	Month	Rainfall (mm/Month)
2010	1	151	2013	1	204	2016	1	137
	2	73		2	289		2	124
	3	147		3	88		3	57
	4	206		4	188		4	77
	5	232		5	191		5	237
	6	231		6	126		6	185
	7	213		7	159		7	182
	8	181		8	171		8	162
	9	202		9	230		9	215
	10	218		10	315		10	275
	11	333		11	287		11	305
	12	363		12	432		12	370
2011	1	327	2014	1	166	2017	1	408
	2	50		2	23		2	149
	3	368		3	90		3	203
	4	158		4	153		4	259
	5	193		5	264		5	245
	6	151		6	136		6	156
	7	114		7	150		7	169
	8	198		8	217		8	248
	9	220		9	179		9	281
	10	388		10	292		10	247
	11	384		11	355		11	433
	12	392		12	643		12	271
2012	1	238	2015	1	134	2018	1	442
	2	146		2	71		2	74
	3	262		3	11		3	140
	4	230		4	201		4	164
	5	239		5	181		5	236
	6	97		6	163		6	172
	7	152		7	133		7	149
	8	187		8	242		8	123
	9	239		9	210		9	218
	10	254		10	247		10	330
	11	260		11	340		11	279
	12	492		12	226		12	360

Table A3. Monthly rainfall in Peninsula Malaysia from 2019 to 2020 [64].

Year	Month	Rainfall (mm/Month)
2019	1	164
	2	68
	3	92
	4	167
	5	236
	6	210
	7	108
	8	148
	9	149
	10	320
	11	274
	12	261
2020	1	108
	2	121
	3	110
	4	262
	5	241
	6	249
	7	275
	8	142
	9	246
	10	213
	11	401
	12	360

Appendix B

Using M70 dataset as a calculation example, the optimum λ value was identified to be 0.049 (Table 7). Substituting it into Equation (1) to obtain:

$$Q_{0.049} = \frac{(P - 0.049S_{0.049})^2}{P - 0.049S_{0.049} + S_{0.049}}$$

Substituting Equation (6) into $S_{0.049}$ in above will yield:

$$Q_{0.049} = \frac{\left[P - 0.049\left(1.184{S_{0.2}}^{1.081}\right)\right]^2}{P + 0.951\left(1.184{S_{0.2}}^{1.081}\right)}$$

Substituting $S_{0.2} = (25{,}400/\mathrm{CN}_{0.2}) - 254$ into $S_{0.2}$ in above to obtain:

$$Q_{0.049} = \frac{\left[P - 0.049\left\{1.184\left(\frac{25{,}400}{\mathrm{CN}_{0.2}} - 254\right)^{1.081}\right\}\right]^2}{P + 0.951\left\{1.184\left(\frac{25{,}400}{\mathrm{CN}_{0.2}} - 254\right)^{1.081}\right\}}$$

$$Q_{0.049} = \frac{\left[P - 23.077\left(\frac{100}{\mathrm{CN}_{0.2}} - 1\right)^{1.081}\right]^2}{\left[P + 447.876\left(\frac{100}{\mathrm{CN}_{0.2}} - 1\right)^{1.081}\right]} \quad \text{(A1)}$$

Equation (A1) is also subject to the constraint $P > 0.049S_{0.049}$

Or $P > 23.077\left(\frac{100}{\mathrm{CN}_{0.2}} - 1\right)^{1.081}$ else $Q_{0.049} = 0$

P = Rainfall depth (mm)

$\mathrm{CN}_{0.2}$ = Conventional SCS tabulated curve number

$Q_{0.049}$ = Runoff depth (mm) of λ = 0.049 for M70 dataset.

References

1. Akomolafe, G.F.; Rosazlina, R. Land use and land cover changes influence the land surface temperature and vegetation in Penang Island, Peninsular Malaysia. *Sci. Rep.* **2022**, *12*, 21250. [CrossRef] [PubMed]
2. Wong, C.L.; Liew, J.; Yusop, Z.; Ismail, T.; Venneker, R.; Uhlenbrook, S. Rainfall characteristics and regionalization in Peninsular Malaysia based on a high resolution gridded data set. *Water* **2016**, *8*, 500. [CrossRef]
3. Baig, M.F.; Mustafa, M.R.U.; Baig, I.; Takaijudin, H.B.; Zeshan, M.T. Assessment of land use land cover changes and future predictions using CA-ANN simulation for Selangor, Malaysia. *Water* **2022**, *14*, 402. [CrossRef]
4. Abdul Rahim, N.; Zulkifli, Y. Hydrological impacts of forestry and land use activities: Malaysian and regional experience. In *Paper Presented at the Seminar on Water, Forestry and Land Use Perspectives*; Forest Research Institute Malaysia: Kepong, Malaysia, 1999.
5. Bonell, M. Selected issues in mountain hydrology of the humid tropics. In *Water: Forestry and Land Use Perspectives*; IHP-VI/Technical document in Hydrology; UNESCO: Paris, France, 2004; pp. 34–56.
6. Bruijnzeel, L.A.; Bonell, M.; Gilmour, D.A.; Lamd, D. Conclusion: Forest water and people in the humid tropics: An emerging view. In *Forest, Water and People in the Humid Tropics; Past, Present and Future Hydrological Research for Integrated Land and Water Management*; Cambridge University Press: Paris, France, 2005; pp. 906–925.
7. Hall, A.L. People in tropical forest: Problem or solutions? In *Forest, Water and People in the Humid Tropics; Past, Present and Future Hydrological Research for Integrated Land and Water Management*; Cambridge University Press: Paris, France, 2005; pp. 75–85.
8. Murdiyarso, D. Water resources management policy responses to land cover change in South East Asian River basins. In *Forest, Water and People in the Humid Tropics; Past, Present and Future Hydrological Research for Integrated Land and Water Management*; Cambridge University Press: Paris, France, 2005; pp. 121–133.
9. Calder, I.R. *The Blue Revolution: Land Use and Integrated Water Resources Management*; Earthscan Publications Ltd.: London, UK, 1999.
10. Velaquez, A.; Duran, E.; Ramirez, I.; Mas, J.F.; Bocco, G.; Ramirez, G.; Palacio, J.L. Land use-cover change processes in highly biodiverse areas: The case of Qaxaca, Mexico. *Glob. Environ. Chang.* **2003**, *13*, 175–184. [CrossRef]
11. Yunus, A.J.M.; Nakagoshi, N.; Ibrahim, A.L. Riparian land use and land cover change analysis using GOS in Pinang River watershed, Malaysia. *Tropics* **2004**, *13*, 235–248. [CrossRef]
12. Miyamoto, M.; Parid, M.M.; Aini, Z.N.; Michinaka, T. Proximate and underlying causes of forest cover change in Peninsula Malaysia. *For. Policy Econ.* **2014**, *44*, 18–25. [CrossRef]
13. Hamid, W.A.; Rahman, S.B.W.A. Comparison results of forest cover mapping of Peninsular Malaysia using geospatial technology. *IOP Conf. Ser. Earth Environ. Sci.* **2016**, *37*, 012027. [CrossRef]
14. Kamlisa, U.K.; Renate, B.A.; Mui-How, P. Monitoring deforestation in Malaysia between 1985 and 2013: Insight from South-Western Sabah and its protected peat swamp area. *Land Use Policy* **2016**, *57*, 418–430.
15. Mohd Jaafar, W.S.W.; Maulud, K.N.A.; Kamarulzaman, A.M.M.; Raihan, A.; Md Sah, S.; Ahmad, A.; Saad, S.N.M.; Mohd Azmi, A.T.; Syukri, N.K.A.J.; Khan, W.R. The influence of deforestation on land surface temperature—A case study of Perak and Kedah, Malaysia. *Forests* **2020**, *11*, 670. [CrossRef]
16. Geography > Area > Total: Countries Compared. Available online: https://www.nationmaster.com/country-info/stats/Geography/Area/Total (accessed on 15 October 2021).
17. Malaysia. Available online: https://www.globalforestwatch.org/ (accessed on 15 October 2021).
18. Department of Forestry, Malaysia. *Annual forestry Report 1997*; Ministry of Science Technology and the Environment: Kuala Lumpur, Malaysia, 1998.
19. Ngah, M.S.Y.C.; Othman, Z. Impact of land development on water quantity and water quality in Peninsular Malaysia. *Malaysian J. Environ. Manag.* **2011**, *12*, 113–120.
20. Hamilton, L.S.; King, P.N. *Tropical Forested Watershed: Hydrologic and Soils Responses to Major Uses of Conversion*; Wesview Press Inc.: Boulder, CO, USA, 1983.
21. Hamilton, L.S.; Pearce, A.J. *What Are the Soil and Water Benefits of Planting Trees in Developing Countries Watershed? Sustainable Resources Development in The Third World*; Westview Press: Boulder, CO, USA, 1987.
22. Hutjes, R.W.A.; Wierda, A.; Veen, A.W.L. Rainfall interception in the Tai Forest, Ivory Coast: Application of two simulation model to a humid tropical system. *J. Hydrol.* **1990**, *114*, 259–275. [CrossRef]
23. Sinun, W.; Wong, W.M.; Douglas, I.; Spencer, T. Throughfall, stemflow, overland flow and throughflow in the Ulu Segama rain forest, Sabah, Malaysia. *Phil. Tran. R. Soc.* **1992**, *335*, 389–395.
24. Asdak, C.; Jarvis, P.G.; Gardingen, P.V.; Fraser, A. Rainfall interception loss in unlogged and logged forest areas of Central Kalimantan, Indonesia. *J. Hydrol.* **1998**, *206*, 237–244. [CrossRef]
25. Calder, I.R. The influence of land use on water yield in upland areas of the UK. *J. Hydrol.* **1986**, *88*, 201–212. [CrossRef]
26. Abdul Rahim, N.; Saifuddin, S.; Zulkifli, Y. Water balance and hydrological characteristics of forested watersheds in Peninsular Malaysia. In Proceedings of the 2nd International Study Conference on GEWEX in Asia and GAME, Pattaya, Thailand, 6–10 March 1995.

27. Abdul Rahim, N.; Baharuddin, K. *Hydrologic Regime of Dipterocarp Forest Catchments in Peninsular Malaysia*; Hydrology Workshop; Universiti Kebangsaan Malaysia: Kota Kinabalu, Malaysia, 1986.
28. Abdul Rahim, N. Water yield changes after forest conversion to agricultural land use in Peninsular Malaysia. *J. Trop. Sci.* **1988**, *1*, 67–84.
29. Zulkifli, Y. Effect of selective logging methods on dissolved nutrient export in Berembun Watershed, Peninsular Malaysia. In Proceedings of the Regional Seminar on Tropical Forest Hydrology, Kuala Lumpur, Malaysia, 4–9 September 1989.
30. Bruijnzeel, L.A. *Hydrology of Moist Tropical Forests and Effects of Conversion: A State of Knowledge Review*; UNESCO IHP Tropic Programme; UNESCO: Paris, France, 1990.
31. Bruijnzeel, L.A. Land use and hydrology in warm humid region: Where do we stand? *IAHS* **1993**, *216*, 1–34.
32. Bonell, M. Progress in the understanding of runoff generation dynamics in forest. *J. Hydrol.* **1993**, *150*, 217–275. [CrossRef]
33. Bonell, M. Tropical Forest hydrology and the role of UNESCO International Hydrological programme. *HESS* **1999**, *3*, 451–461. [CrossRef]
34. Malmer, A. Hydrological effects and nutrient losses of forest plantation establishment on tropical rainforest land in Sabah, Malaysia. *Water Resour. Res.* **1996**, *32*, 2213–2220. [CrossRef]
35. Zhang, P.; Shao, G.; Zhao, G.; Le Master, D.C.; Parker, G.R.; Dunning, J.B., Jr.; Li, Q. China's forest policy for the 21th century. *Science* **2000**, *288*, 2135–2136. [CrossRef]
36. Sharma, K.P.; Vorosmarty, C.J.; Moore, B. Sensitivity of the Himalayan hydrology to land-use and climate changes. *Clim. Chang.* **2000**, *47*, 117–139. [CrossRef]
37. Lazaro, T.R. *Urban Hydrology: A Multidisciplinary Perspective*; Revised Edition; Technomic Publishing Company, Inc.: Lancaster, UK, 1990.
38. High Deforestation Rates in Malaysian States Hit by Flooding. Available online: https://news.mongabay.com/2015/01/high-deforestation-rates-in-malaysian-states-hit-by-flooding/ (accessed on 15 October 2021).
39. Bosch, J.M.; Hewlett, J.D. A review of catchment experiments to determine the effect of vegetation changes on water yield and evapotranspiration. *J. Hydrol.* **1982**, *55*, 3–23. [CrossRef]
40. Brown, A.G.; Nambiar, E.K.S.; Cossalter, C. Plantations for the tropics: Their role, extent and nature. In *Management of Soil, Nutrients and Water in the Tropical Plantation Forests*; Nambiar, E.K.S., Brown, A.G., Eds.; Australian Centre for International Agricultural Research: Canberra, Australia; pp. 1–23.
41. Sidle, R.C.; Sasaki, S.; Otsuki, M.; Noguchi, S.; Abdul Rahim, N. Sediment pathways in a tropical forest: Effects of logging roads and skid trails. *Hydrol. Proc.* **2004**, *18*, 703–720. [CrossRef]
42. Adnan, N.A.; Atkinson, P.M.; Yusoff, Z.M.; Rasam, A.R.A. Climate variability and anthropogenic impacts on a semi-distributed monsoon catchment runoff simulations. In Proceedings of the International Colloquium on Signal Processing & Its Applications, CSPA, Kuala Lumpur, Malaysia, 7–9 March 2014; pp. 178–183.
43. Jourgholami, M.; Karami, S.; Tavankar, F.; Monaco, A.L.; Picchio, R. Effects of slope gradient on runoff and sediment yield on machine-induced compacted soil in temperate forests. *Forests* **2021**, *12*, 49. [CrossRef]
44. Hu, P.; Cai, T.; Sui, F.; Duan, L.; Man, X.; Cui, X. Response of runoff to extreme land use change in the permafrost region of Northeastern China. *Forests* **2021**, *12*, 1021. [CrossRef]
45. Liu, X.Z.; Kang, S.Z.; Liu, L.D.; Zhang, X.P. SCS model based on geographic information and its application to simulate rainfall-runoff relationship at typical small watershed level in Loess Plateau. *Tran. CSAE* **2005**, *21*, 93–97.
46. Baltas, E.A.; Dervos, N.A.; Mimikou, M.A. Technical note: Determination of the SCS initial abstraction ratio in an experimental watershed in Greece. *HESS* **2007**, *11*, 1825–1829. [CrossRef]
47. Mansor, S.; Saadatkhah, N.; Khuzaimah, Z. Regional modelling of rainfall-induced runoff using hydrological model by incorporating plant cover effects: Case study in Kelantan, Malaysia. *Nat. Hazards* **2018**, *93*, 739–764. [CrossRef]
48. Sahin, V.; Hall, M.J. The effects of afforestation and deforestation on water yields. *J. Hydrol.* **1996**, *178*, 293–309. [CrossRef]
49. Ling, L.; Yusop, Z.; Yap, W.S.; Tan, W.L.; Chow, M.F.; Ling, J.L. A calibrated, watershed-specific SCS-CN method: Application to Wangjiaqiao watershed in the three gorges area, China. *Water* **2019**, *12*, 60. [CrossRef]
50. Ling, L.; Yusop, Z.; Ling, J.L. Statistical and Type II Error Assessment of a Runoff Predictive Model in Peninsula Malaysia. *Mathematics* **2021**, *9*, 812. [CrossRef]
51. Hawkins, R.H.; Ward, T.J.; Woodward, D.E.; Vanmullem, J.A. *Progress Report: ASCE Task Committee on Curve Number Hydrology. Managing Watersheds for Human and Natural Impacts*; ASCE: New York, NY, USA, 2005; pp. 1–12.
52. DID, Hydrological Procedure No. 27. Design Flood Hydrograph Estimation for Rural Catchments in Peninsula Malaysia. JPS, DID, Kuala Lumpur. 2010. Available online: https://www.water.gov.my/jps/resources/PDF/Hydrology%20Publication/Hydrological_Procedure_No_27_(HP_27).pdf (accessed on 19 October 2021).
53. Forestry Department Peninsular Malaysia. *Forestry Statistics Peninsular Malaysia 1971–1978*; Forestry Department Peninsular Malaysia: Kuala Lumpur, Malaysia, 1979.
54. Forestry Department Peninsular Malaysia. *Forestry Statistics Peninsular Malaysia 1993*; Forestry Department Peninsular Malaysia: Kuala Lumpur, Malaysia, 1994.
55. Forestry Department Peninsular Malaysia. *Forestry Statistics Peninsular Malaysia 1995*; Forestry Department Peninsular Malaysia: Kuala Lumpur, Malaysia, 1996.

56. Forestry Department Peninsular Malaysia. *Forestry Statistics Peninsular Malaysia 2000*; Forestry Department Peninsular Malaysia: Kuala Lumpur, Malaysia, 2001.
57. Forestry Department Peninsular Malaysia. *Forestry Statistics Peninsular Malaysia 2005*; Forestry Department Peninsular Malaysia: Kuala Lumpur, Malaysia, 2006.
58. Forestry Department Peninsular Malaysia. *Forestry Statistics Peninsular Malaysia 2009*; Forestry Department Peninsular Malaysia: Kuala Lumpur, Malaysia, 2010.
59. Forestry Department Peninsular Malaysia. *Forestry Statistics Peninsular Malaysia 2010*; Forestry Department Peninsular Malaysia: Kuala Lumpur, Malaysia, 2011.
60. Hawkins, R.H. Curve Number Method: Time to Think Anew? *J. Hydrol. Eng.* **2014**, *19*, 1059. [CrossRef]
61. Davidsen, S.; Löwe, R.; Ravn, N.H.; Jensen, L.N.; Arnbjerg-Nielsen, K. Initial conditions of urban permeable surfaces in rainfall-runoff models using Horton's infiltration. *Water Sci. Technol.* **2017**, *77*, 662–669. [CrossRef] [PubMed]
62. Downloading IBM SPSS Statistics 26. Available online: https://www.ibm.com/support/pages/downloading-ibm-spss-statistics-26 (accessed on 15 October 2021).
63. Hawkins, R.H.; Ward, T.J.; Woodward, D.E.; Van Mullem, J. *Curve Number Hydrology: State of the Practice*; ASCE: Reston, VA, USA, 2009.
64. Huffman, G.J.; Stocker, E.F.; Bolvin, D.T.; Nelkin, E.J.; Tan, J. *GPM IMERG Final Precipitation L3 1 Month 0.1 Degree x 0.1 Degree V06*; Goddard Earth Sciences Data and Information Services Center (GES DISC): Greenbelt, MD, USA, 2019.
65. Giovanni. Available online: https://giovanni.gsfc.nasa.gov/giovanni/ (accessed on 15 October 2021).
66. Jiang, R.Y. Investigation of Runoff Curve Number Initial Abstraction Ratio. Master's Thesis, The University of Arizona, Tucson, AZ, USA, 2001.
67. Woodward, D.E.; Hawkins, R.H.; Jiang, R.; Hjelmfelt, A.T.; Van Mullem, J.A.; Quan, Q.D. Runoff curve number method: Examination of the initial abstraction ratio. In Proceedings of the World Water and Environmental Resources Congress, Philadelphia, PA, USA, 23–26 June 2003; pp. 1–10.
68. Hawkins, R.H.; Ward, T.J.; Woodward, D.E.; Van Mullem, J.A. Continuing Evolution of Rainfall-Runoff and the Curve Number Precedent. In Proceedings of the 2nd Joint Federal Interagency Conference Proceeding, Las Vegas, NV, USA, 27 June–1 July 2010; pp. 1–12.
69. Ponce, V.M.; Hawkins, R.H. Runoff Curve Number: Has it Reached Maturity? *J. Hydrol.* **1996**, *1*, 11–19. [CrossRef]
70. Hawkins, R.H.; Khojeini, A.V. Initial abstraction and loss in the curve number method. In Proceedings of the Arizona State Hydrological Society Proceedings, Las Vegas, NV, USA, 15–17 April 2000; pp. 115–119.
71. Kim, N.W.; Lee, J.; Lee, J.E. SWAT application to estimate design runoff curve number for South Korean conditions. *Hydrol. Proc.* **2010**, *24*, 2156–2170. [CrossRef]
72. Boughton, W.C. A Review of the USDA SCS Curve Number Method. *Aust. J. Soil Res.* **1989**, *27*, 511–523. [CrossRef]
73. McCuen, R.H. Approach to confidence interval estimation for curve numbers. *J. Hydrol.* **2002**, *1*, 43–48. [CrossRef]
74. Hawkins, R.H. Improved Prediction of Storm Runoff in Mountain Watersheds. *J. Irrig. Drain. Eng. ASCE* **1973**, *99*, 519–523. [CrossRef]
75. Zevenbergen, A.T. *Runoff Curve Numbers for Rangelands from Rangeland from Landsat Data*; Technical Rep, HL85-1; U.S. Department of Agriculture Research Service, Hydraulic Laboratory: Beltsville, MD, USA, 1985.
76. Sneller, J.A. *Computation of Runoff Curve Numbers for Rangelands from Landsat Data*; Technical Rep, HL85-2; U.S. Department of Agriculture Research Service, Hydraulic Laboratory: Beltsville, MD, USA, 1985.
77. Hawkins, R.H. Asymptotic determination of runoff curve numbers from data. *J. Irrig. Drain. Eng. ASCE* **1993**, *119*, 334–345. [CrossRef]
78. Van Mullen, J.A. Runoff and peak discharges using Green–Ampt infiltration model. *J. Hydr. Eng. Div.-ASCE* **1991**, *117*, 354–370. [CrossRef]
79. Official Website Forestry Department of Peninsular Malaysia. Available online: https://www.forestry.gov.my/en/2016-06-07-02-53-46/2016-06-07-03-12-29 (accessed on 15 October 2021).
80. Cheng, M.H. The Impact of Ethnicity on the Regional Economic Development in Malaysia. Master's Thesis, Hiroshima University, Hiroshima, Japan, 2011.
81. Department of Statistics, Malaysia. *General Report of the Population Census of Malaysia 1970*; Department of Statistics, Malaysia: Kuala Lumpur, Malaysia, 1977; Volume 1.
82. Department of Statistics, Malaysia. *General Report of the Population Census of Malaysia 1991*; Department of Statistics, Malaysia: Kuala Lumpur, Malaysia, 1995; Volume 1.
83. Department of Statistics, Malaysia. *Preliminary Count Report for Urban and Rural Areas*; Department of Statistics, Malaysia: Kuala Lumpur, Malaysia, 2001.
84. Department of Statistics, Malaysia. *Population Distribution and Basic Demographic Characteristics*; Department of Statistics, Malaysia: Kuala Lumpur, Malaysia, 2001.
85. Department of Statistics, Malaysia. *Migration Survey Report Malaysia 2007*; Department of Statistics, Malaysia: Putrajaya, Malaysia, 2009.
86. Department of Statistics, Malaysia. *Preliminary Count Report 2010*; Department of Statistics, Malaysia: Putrajaya, Putrajaya, Malaysia, 2010.

87. Department of Statistics, Malaysia. *Population Distribution by Local Authority Areas and Mukims*; Department of Statistics, Malaysia: Putrajaya, Malaysia, 2011.
88. Iya, S.G.D.; Gasim, M.B.; Toriman, M.E.; Abdullahi, M.G. Floods in Malaysia: Historical reviews, causes, effects and mitigations approach. *Int. J. Interdiscip. Res. Innov.* **2014**, *2*, 59–65.
89. Malaysia Flood List. Available online: https://floodlist.com/tag/malaysia (accessed on 18 October 2021).
90. When Forest can no Longer Prevent Floods. Available online: https://themalaysianreserve.com/2021/01/11/when-forest-can-no-longer-prevent-floods/ (accessed on 18 October 2021).
91. Deforestation the Cause of Flood. Available online: https://www.thestar.com.my/opinion/letters/2014/11/08/deforestation-the-cause-of-flood (accessed on 18 October 2021).
92. Deforestation Likely Behind Deadly Sabah Mudslide, Says Expert. Available online: https://www.nst.com.my/news/2017/04/227539/deforestation-likely-behind-deadly-sabah-mudslide-says-expert (accessed on 18 October 2021).
93. Akter, A.; Mohd Noor, M.J.M.; Goto, M.; Khanam, S.; Parvez, A.; Rasheduzzaman, M. Landslide disaster in Malaysia: An overview. *Int. J. Innov. Res.* **2019**, *8*, 292–302. [CrossRef]
94. Majid, N.A.; Taha, M.R.; Selamat, S.N. Historical landslide events in Malaysia 1993–2019. *Indian J. Sci. Technol.* **2020**, *13*, 3387–3399. [CrossRef]